

03,13

Effect of the thickness on electrical resistance of thin diamond-like carbon coatings on silicon substrate

© I.A. Zur^{1,2}, E.E. Shmanay^{1,3}, Y.A. Fedotova¹, A.A. Kharchanka¹, S.A. Movchan⁴

¹ Institute for Nuclear Problems, Belarusian State University, Minsk, Belarus

² Department of Energy Physics of the Belarusian State University, Minsk, Belarus

³ Department of Micro- and Nanoelectronics of the Belarusian State University of Informatics and Radioelectronics, Minsk, Belarus

⁴ Joint Institute for Nuclear Research, Dubna, Moscow oblast, Dubna, Russia

E-mail: zur.ilya01@gmail.com

Received August 26, 2022

Revised August 26, 2022

Accepted September 3, 2022

The relationship between sp^2/sp^3 -hybridizations ratio of atomic bonds in diamond-like carbon (*DLC* — Diamond-Like Carbon) and its electrical resistivity for coatings with a thickness in the range 22–70 nm prepared by vacuum arc deposition on silicon substrate of the KDB-8 brand has been established. It is established, that an increase in the coating thickness from 22 to 70 nm is accompanied by a decrease in the specific transverse electrical resistance of samples from 17 to $2\text{ G}\Omega \cdot \text{m}$. This effect is explained by an increase in the proportion of carbon atoms with sp^2 -hybridization of electronic orbitals from 86 to 91%, which leads to the appearance of an additional number of π -bonds. A mathematical model, describing the spatial distribution of current when measuring transverse I-V characteristic, has been developed. The results obtained will be useful in creating resistive layers on the electrodes of gas-discharge detectors of charged particle to limit the amount of current in the event of rare spark discharges inside them caused by the registration of random highly ionizing particles.

Keywords: (*DLC*), electrical properties of thin films, hybridization of electronic orbitals, Raman scattering, I-V characteristic.

DOI: 10.21883/PSS.2023.01.54973.457

1. Introduction

Improving the functional characteristics of gas-discharge detectors is an important task for various fields of science and technology, including in modern experimental particle physics, the increasing role of which is inextricably linked with progress in the field of detector technologies [1–2]. In this regard, it seems urgent to increase the stability of gas electronic multipliers to breakdowns [3], that occur when registering strongly ionizing particles from for exceeding the Reter limit (10^7) [4].

One of the methods of increasing the resistance of gas-discharge detectors to breakdown is the application of resistive coatings [5–11] to the electrodes, which prevent the development of the arc stage of breakdown by locally reducing the voltage in the gas gain region. As such coatings, various scientific groups have studied carbon resistive films [5,7,10], *DLC*-coatings [6–9,11], coatings CuO and CrO [12].

According to the research results in [6,12], μ -WELL detectors with a resistive *DLC*-coating of an anode electrode with a surface resistance in the range from 10 to $100\text{ M}\Omega/\text{sq}$ demonstrated an increase in the gain in a stable mode relative to detectors without the appropriate coating.

In gas-discharge detectors *DLC*-coatings are deposited on polymer substrates (lavsan, kapton), which makes it impossible to use the Raman spectroscopy to study the chemical bonds of atoms in coatings (the content of carbon atoms with sp^2 - and sp^3 - by hybridization of σ -links). Coatings deposited on a silicon substrate (Si) are optimal for studying the structure of *DLC*, however, for such samples, due to the significantly greater electrical conductivity of the substrate, only the measurement of the transverse electrical resistance of the *DLC*-coating, which determines the most important parameter of resistive coatings for detectors — will be correct. surface electrical resistance.

The aim of the work is to determine the specific transverse electrical resistance and to establish the influence on it of the ratio of the fractions of atoms located in sp^2 - and sp^3 -hybridized state in the *DLC*-coatings.

2. Methods of synthesis and research of samples

Samples of *DLC*-coatings were deposited on silicon substrates of the KDB grade-8 (hereinafter *DLC*//Si) on

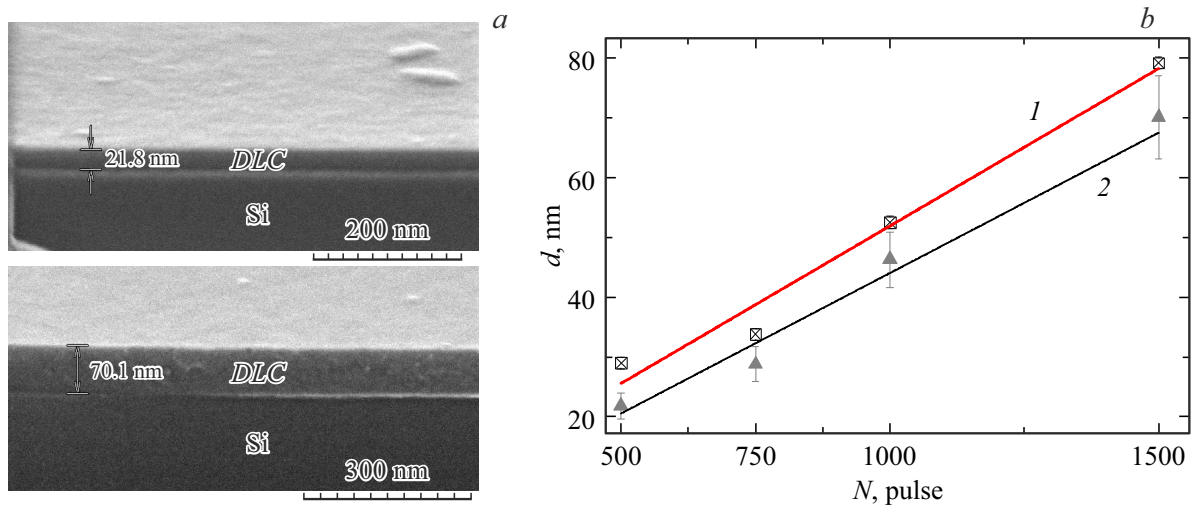


Figure 1. SAM-cross-sectional images for samples *DLC*//*Si* obtained using $N = 500$ and $N = 1500$ pulse (a); thickness dependences d on the number of pulses N measured on *DLC*-coatings by (1) ellipsometry and (2) SAM on cross sections (b).

the *PVM-D* installation by vacuum arc method [14] with a pulsed electric arc evaporator at a pulse repetition frequency of 3 Hz, an operating pressure in the chamber of $\sim 10^{-3}$ Pa and a substrate temperature of about 350 ± 17 K. To improve the adhesive ability of the coating, the surface of the substrates was cleaned with argon ions with an average energy of 75 eV from undesirable organic compounds with a duration of 5 min. To increase the uniformity of the *DLC*-coating in thickness during deposition, the rotation of the samples relative to the evaporator was used. The thickness of the samples d was controlled by counting the number of voltage pulses N on the cathode-arc evaporator; for the resulting series of samples N it was 500, 750, 1000 and 1500.

To identify the type of chemical bonds of carbon atoms in the samples, the Raman spectra obtained using a HORIBA XploRA PLUS confocal Raman microscope with an exciting laser wavelength of 532 nm were analyzed.

The electrical conductivity properties of the *DLC*-coatings were characterized by a differential electrical resistance $R = dE/dj$, which was determined from the transverse volt-ampere characteristics (VAC), where j — the transverse current density, $E = U/d$ — the strength of the transverse offset field without taking into account the bending of the zones at the boundary *DLC*-silicon. The VAC was recorded using the Agilent 4156 semiconductor device parameter analyzer using a two-probe direct current method. Tungsten needles were used as pressure contacts.

To obtain the dependence of the $d(N)$ thickness of the *DLC* coating on the number of current pulses N in an electric arc evaporator, cross-sectional images of samples *DLC*//*Si* obtained on a scanning electron microscope (SEM) *HITACHI S-4800* were analyzed. Additionally, in order to verify the SEM data, the thickness of the coatings

was estimated using ellipsometry at the LEF-3M-1 installation.

The system of equations for a mathematical model describing the distribution of the current density j over the cross-section of the sample when measuring the VAC was solved by the finite element method using the module *AC/DC* of the software *COMSOL 5.6*.

3. Experimental procedure

3.1. Determining the coating thickness *DLC*

In Fig. 1, a, examples of typical SEM images of cross-sections of the thinnest (obtained at $N = 500$) and the thickest ($N = 1500$) samples are presented. The contrast distribution on the SEM-images indicates an increase in the thickness of the *DLC*-coating with an increase in the number of pulses N in the range from ~ 22 nm to ~ 70 nm (the curve in Fig. 1, b). Ellipsometry data confirmed the nature of the change in the dependence $d(N)$, showing an increase in the thicknesses from 29 to 79 nm. Thus, independent methods of thickness analysis gave close values $d(N)$, which indicates the correctness of their estimation. Fig. 1, b, shows the dependences of the thickness of the *DLC*-coating, determined from the ellipsometry data (1) and SEM (2), on the number of pulses N , which can be with a good degree the accuracy is approximated by a linear function.

3.2. Raman spectroscopy

When analyzing the proportion of sp^2 - and sp^3 - of hybridized bonds between carbon atoms in *DLC*//*Si* samples, in accordance with the method described in the work [15], the position and the ratio of the intensities G (*Graphite-like*) and D (*Disordered*) peaks, which are

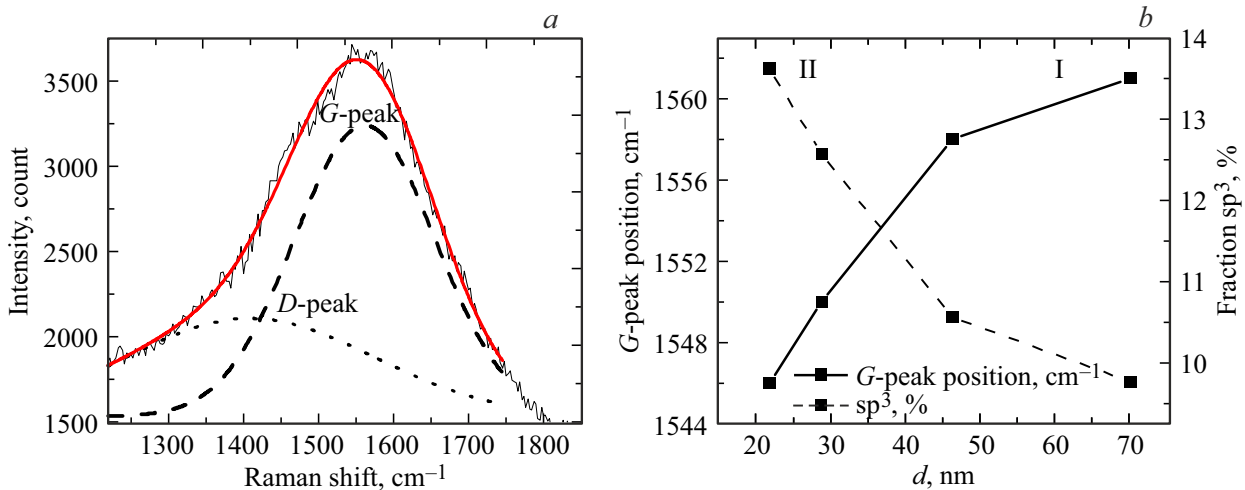


Figure 2. *a* — Raman and Fourier spectrum-subspectrals for the sample *DLC//Si* thickness $d = 70$ nm; *b* — dependences of the position *G* of the peak (I) and the percentage of carbon atoms in the sp^3 -hybridized state (II) of the film thickness.

caused by the presence of stretching vibrations in the carbon ring with E_{2g} -symmetry and „of respiratory“ vibrations with A_{1g} -symmetry, respectively. A characteristic view of the Raman spectrum for a sample with $N = 1500$ pulse is shown in Figure 2, *a*. To determine the positions *G* and *D* of the peaks, the initial spectra were deconvoluted by the Gaussian function:

$$y = y_0 + \frac{A}{w\sqrt{\pi/2}} \exp \left[-2 \frac{(x - x_c)^2}{w^2} \right], \quad (1)$$

where x_c and w are the centroid and the full width of the peak at half height, y_0 and A are the distribution parameters.

It was found that with an increase in the film thickness from 22 to 70 nm, the position of the *G*-peak monotonically shifts from 1546 to 1562 cm^{-1} , as shown in Fig. 2, *b*, curve I. Figure 2, *b*, curve II, presents an estimate of the percentage of carbon atoms in the sp^3 -hybridized state, made based on the results of the work [16]. It can be seen from the curve II that an increase in the film thickness d is accompanied by a decrease in the proportion of carbon atoms in the sp^3 -hybridized state, which, accordingly, leads to an increase in the number of π -bonds, which can increase the specific electrical conductivity of coatings.

3.3. Volt-ampere characteristics of the structure *W//DLC//Si//W* at room temperature

Volt-ampere characteristics allow us to investigate the features of charge carrier transport in materials. As can be seen from Fig. 3, *a*, the transverse VAC structures *W//DLC//Si//W*, consisting of samples and tungsten contacts (*W*), measured at offset voltages in the range from -5 to 5 V, are nonlinear and asymmetric. In addition, during the measurements, a certain offset relative to zero on the stress scale was observed, not exceeding 0.1 V, which was

Barrier value φ_b samples *DLC//Si* for the quantity of pulses N equal to 500, 750, 1000 and 1500

Sample	22 nm	28 nm	46 nm	70 nm
Barrier value φ_b	34.07 kT	33.61 kT	33.62 kT	33.46 kT

centered for the correctness of the analysis. The nonlinearity and asymmetry of the VAC can be caused by the formation of Schottky barriers at the boundaries of the needle-silicon and needle-*DLC*: the electron output work for tungsten is 4.5 eV [17], for boron-doped silicon ≈ 4.3 eV [17], for *DLC* the output work is much smaller and has an order of magnitude of 1 eV [18].

The height of the potential barrier φ_b determines the density of charge carriers injected from the metal into the dielectric. The field dependence of the current density j of the direct branch of the VAC is described by the Richardson–Schottky model (2) and is linearized to the values of the square root of the electric voltage $E^{1/2} = 5 \cdot 10^3$ (V/m) $^{1/2}$ for the thinnest sample $d = 22$ nm and up to $11 \cdot 10^3$ (V/m) $^{1/2}$ for a sample with a thickness of 70 nm, Fig. 3, *b*.

$$j = AT^2 \exp \left(-\frac{\varphi_b - \beta E^{1/2}}{kT} \right) \quad (2)$$

$$\beta = (e^3 / q\pi\epsilon\epsilon_0 d)^{1/2}, \quad (3)$$

where A — Richardson–Deschmann constant, T — sample temperature during measurement, ϵ — permittivity equal to 2.2 for *DLC*, ϵ_0 — vacuum permittivity, k — Boltzmann constant, e — electron charge, d — thickness *DLC*, a — coefficient equal to 4 for the Richardson–Schottky model.

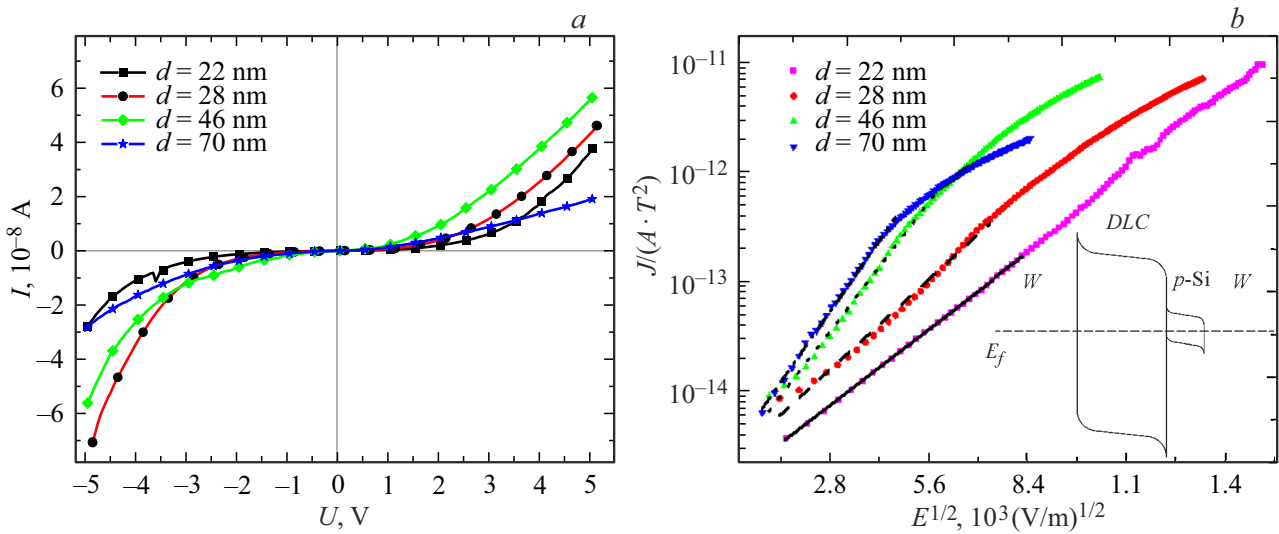


Figure 3. Transverse VAC structures W//DLC//Si//W for samples *DLC* thickness *d* in the range from 22 to 70 nm at a temperature $T = 300$ K: *a* — for the forward and reverse branches; *b* — for the forward branch in coordinates $\ln(j/A \cdot T^2) - E^{1/2}$. In the insert — schematic representation of the zone diagram of the structure W//DLC//Si//W is not in scale.

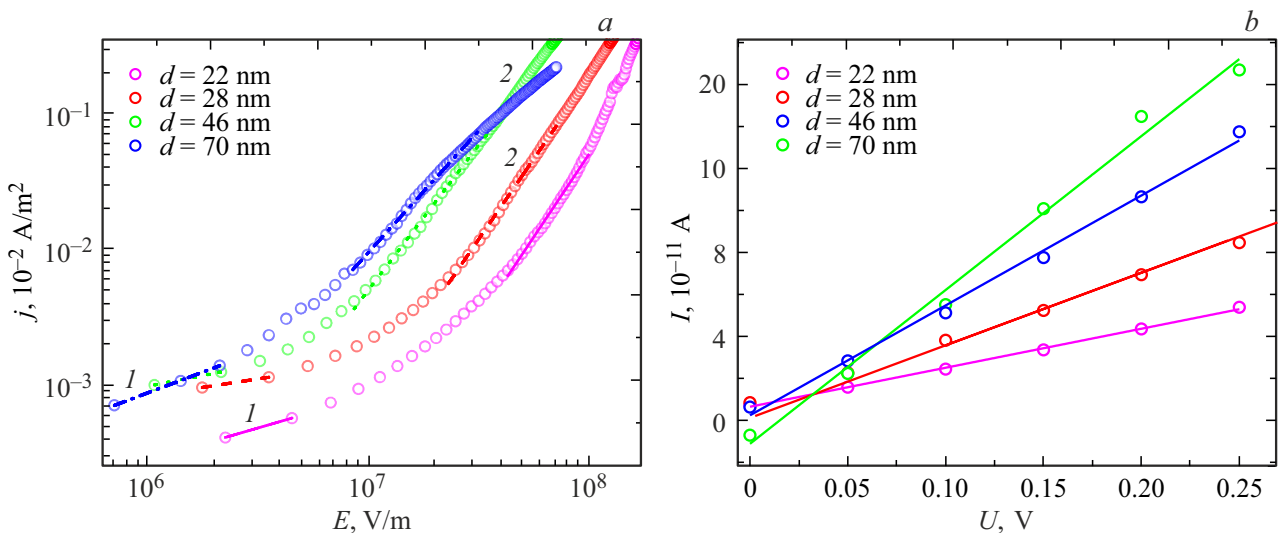


Figure 4. Transverse VAC structures W//DLC//Si//W for samples *DLC* with a thickness of *d* in the range from 22 to 70 nm at a temperature of $T = 300$ K: *a* — the reverse branch of the VAC on a double logarithmic scale; *b* — linearization of the direct branches of the VAC for the voltage range from 0 to 0.25 V.

The value of the potential barrier φ_b for the studied samples, estimated by the Richardson-Schottky model, has values of the order $33 \text{ kT} \sim 0.8 \text{ eV}$ (table). Such values φ_b are close to the Schottky barrier for contacts W/Si [19].

Rebuilding the reverse branch of the VAC in coordinates $\ln(j/AT^2) - E^{1/2}$ does not lead to their linearization in the field area $E < 1.1 \cdot 10^4 \text{ (V/m)}^{1/2}$. However, the rearrangement of $j(E)$ in double logarithmic coordinates, Fig. 4, *a*, leads to two linear sections with different slopes (1 at low E and 2 at higher E). The latter indicates the possibility of describing the reverse VAC model of a current limited by a volumetric charge (the ideal Mott-Gurney model) [20].

4. Numerical determination of the cross section of the current channel and the dependence of the resistivity on the thickness of *DLC*-coatings

The electrical resistivity of *DLC*-coatings was estimated from the resistance formula of a cylindrical sample

$$\rho = \frac{RS}{d}, \quad (4)$$

where R and d — absolute resistance and thickness *DLC*- of the coating, S — cross-sectional area of the current channel.

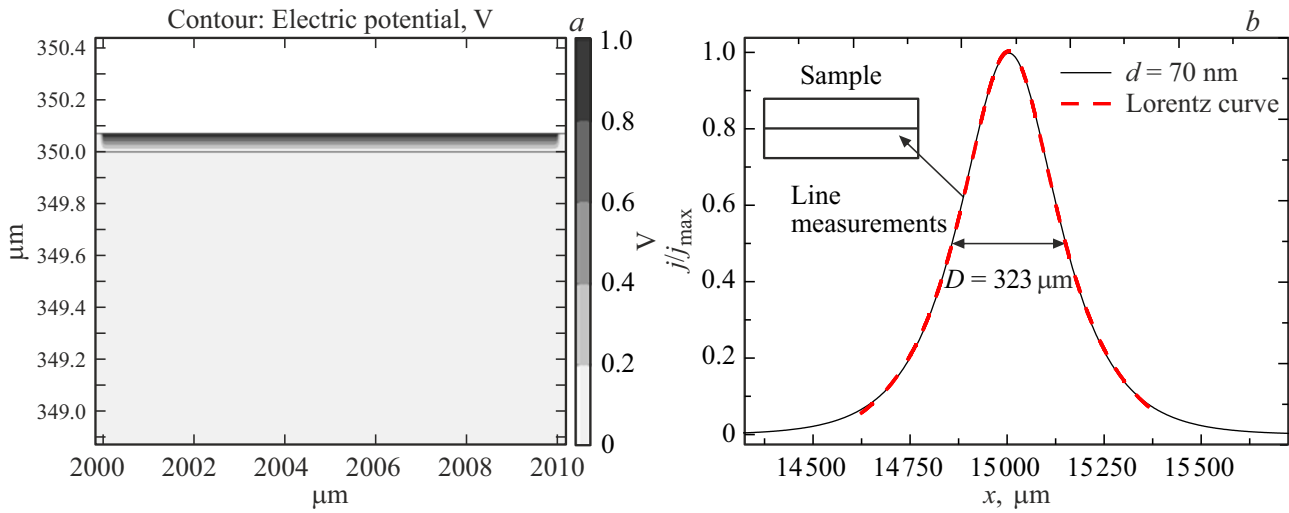


Figure 5. Results of a numerical experiment for a single potential difference for a sample *DLC/Si*: *a* — potential distribution in the sample; *b* — a maximized current density profile in the median section of the sample.

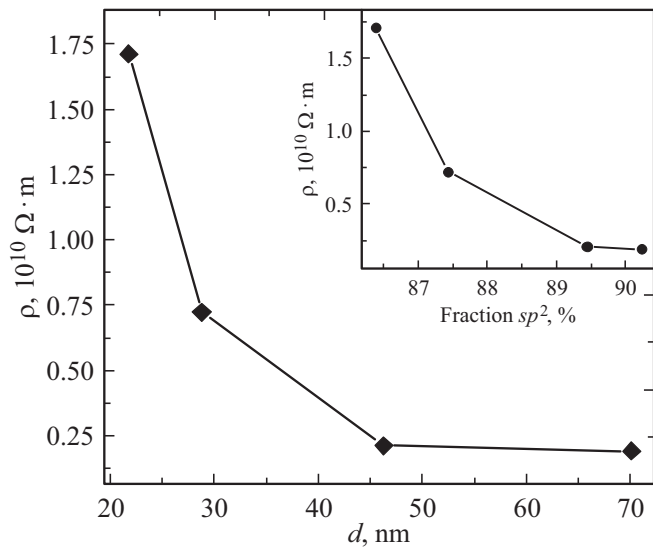


Figure 6. Dependence of the specific transverse electrical resistance ρ on the thickness d *DLC*- of the coating. In the insert — the dependence of the electrical resistivity ρ *DLC*- of the coating on the proportion of sp^2 - of hybridized bonds.

The clamping contacts that are used when recording VAC have a nominal linear size of the order of $10\ \mu\text{m}$, which allows us to consider the contacts as point sources of electric potential, then to estimate the area of the current channel S it is sufficient to know the distribution of currents in the sample.

The mathematical model (5) describing the current density distribution j in the sample consists of the differential Ohm's law and the continuity equation for the electric charge density q , with Dirichlet boundary conditions for the unit and zero potential for the first and second contacts,

respectively.

$$\begin{cases} j = \sigma E \\ E = -\nabla\varphi \\ \nabla \cdot j = -\frac{\partial q}{\partial t} \end{cases}, \quad (5)$$

where σ — specific electrical conductivity of (ρ^{-1}) *DLC*-coating, φ and E — electrostatic potential and electric field strength of offset.

The calculated area consists of a substrate with a thickness of $350\ \mu\text{m}$ and a coating *DLC* with thicknesses d from 22 to 70 nm. The contact area of the measuring needle and the sample has a linear size of $10\ \mu\text{m}$. Fig. 5, *a* shows a map of the potential distribution in the sample with a single interelectrode potential difference. The diameter of the current channel D was estimated as the width at half-height of the Lorentz contour, which approximated the initial values of the current density in the median section of the sample, Fig. 5, *b*.

Knowing the diameter of the channel D with the corresponding area S and the transverse differential electrical resistance R , it is possible to construct the dependence of the specific electrical resistance *DLC*- of the coating ρ on the thickness d , which is shown in Fig. 6.

As can be seen, the obtained experimental values of the electrical resistivity *DLC* are in the range from 2 to $17\ \text{G}\Omega \cdot \text{m}$. According to the literature data [21] the range of resistivity values of *DLC*-coatings is $1 \cdot 10^3 \dots 10^{14}\ \Omega \cdot \text{m}$ for different deposition conditions that affect the ratio of sp^2 - and sp^3 -hybridized σ -bonds. The tendency of decreasing resistivity *DLC* with increasing thickness correlates with its dependence on the proportion of sp^2 - of hybridized bonds between carbon atoms.

5. Conclusion

There has been confirmed the relationship between the proportion of sp^2 - and sp^3 - of hybridized bonds between carbon atoms and the value of electrical resistivity *DLC*-coatings, obtained by vacuum-arc method on silicon substrates of the KDB grade-8.

According to ellipsometry and SEM images of cross-sections of samples *DLC*/Si, an increase in the thickness of the film *DLC* from 22 to 70 nm with an increase in the number of current pulses N from 500 to 1500 in an electric arc evaporator during deposition was proved.

Analysis of Raman spectra revealed that the content of chemical bonds between carbon atoms in the sp^3 -hybridized state decreases from 14 to 9% with an increase in the coating thickness from 22 to 70 nm, which leads to an increase in the amount of π -bonds and, as a consequence, a decrease in the electrical resistivity from 17 to $2\text{ G}\Omega \cdot \text{m}$.

The finite element method obtained the distribution of the potential and current density in the sample when measuring the transverse VAC. The results obtained show that by controlling the thickness of the coating *DLC*, which determines the proportion of carbon atoms in the sp^3 -hybridized state, it is possible to effectively adjust the amount of electrical resistance of the coating to quench breakdowns in gas-discharge charged particle detectors.

Acknowledgments

The authors express their gratitude to prof. A.K. Fedotov, Candidate of Physics.-mat.sci. A.S. Fedotov and researcher of the NIL of Energy-efficient Materials and Technologists of BSU A.V. Baglov for the fruitful scientific discussions and assistance in conducting experiments.

Funding

The study was carried out under the contract „Testing of the technology of controlled application of *DLC* on dielectric substrates for *GEM*-detectors“ No. 08626319/211293539-74 with JINR (Dubna, Russia).

Conflict of interest

The authors declare that they have no conflict of interest.

References

- [1] D. Pierroutsakou. EPJ Web Conf. **184**, 1015 (2018).
- [2] M. Musacci, G. Bigongiari, P. Brogi, C. Checchia, G. Collazuol, G.F. Dalla Betta, A. Ficorella, P.S. Marrocchesi, S. Mattiazzo, F. Morsani, S. Noli, L. Pancheri, L. Ratti, A. Savoy Navarro, L. Silvestrin, F. Stolzi, J. Suh, A. Sulaj, C. Vacchi, M. Zarghami. Nucl. Instrum. Meth. Phys. Res. Sect. Accel. Spectromet. Detect. Assoc. Equip. **936**, 695 (2019).
- [3] A. Breskin D, Mormann, A. Lyashenko, R. Checkik, F.D. Amaro, J.M. Maia J.F.C.A. Veloso, J.M.F. dos Santos. Nucl. Instrum. Meth. Phys. Res. Sect. Accel. Spectromet. Detect. Assoc. Equip. **553**, 46 (2005).
- [4] H. Raether. Electron avalanches and breakdown in gases. Butterworths, Washington (1964).
- [5] T. Alexopoulos, J. Burnens, R. de Oliveira, G. Glonti, O. Pizzirusso, V. Polychronakos, G. Sekhniadze, G. Tsiopolitis, J. Wotschack. Nucl. Instrum. Meth. A **640**, 110 (2011).
- [6] J. Manjarres, T. Alexopoulos, D. Attie, M. Boyer, J. Derre, G. Fanourakis, E. Ferrer-Ribas, J. Galan, E. Gazis, T. Gerasis, A. Giganon, I. Giomataris, S. Herlant, F. Jeanneau, Ph. Schune, M. Titova, G. Tsiopolitis. J. Instrum. **7**, 12071 (2012).
- [7] G. Bencivenn, R. de Oliveira, G. Felici, M. Gatta, M. Giovannetti, G. Morello, A. Ochi, M. Poli Lenera, E. Tskhadadze. J. Instrum. **14**, 5014 (2019).
- [8] A. Kashchuk, V. Akulich, K. Afanaciev, V. Bayev, A. Churakov, N. Kravchuk, N. Kuchinskiy, O. Levitskaya, A.V. Solin, A.A. Solin, S. Movchan, V. Tchekhovski. J. Instrum. **15**, 9, 9041 (2020).
- [9] M. Iodic, M. Alviggi, M.T. Camerlingo, V. Canale, M. Della Pietra, C. DiDonato, P. Iengo, F. Petrucci, G. Sekhniadze. J. Phys. Conf. Ser. **1498**, 1, 12028 (2020).
- [10] V. Peskov, P. Fonte, P. Martinengo, E. Nappi, R. Oliveira, F. Pietropaolo, P. Picchi. Nucl. Instrum. Meth. Phys. Res. Sect. Accel. Spectromet. Detect. Assoc. Equip. **661**, 153 (2012).
- [11] V.G. Bayev, K.G. Afanaciev, S.A. Movchan, A. Gongadze, V.V. Akulich, A.O. Kolesnikov, N. Koviazina, L. Gongadze, R. Sotenskii, I. Minashvili. Nucl. Instrum. Meth. A **1031**, 166528 (2022).
- [12] V. Peskov, B. Baibussinov, S. Centro, A. DiMauro, B. Lund-Jensen, P. Martinengo, E. Nappi, R. Oliveira, F. Pietropaolo, P. Picchi, L. Periale, I. Rodionov, S. Ventura. IEEE Trans. Nucl. Sci. **54**, 5, 1784 (2007).
- [13] I. Vankov. Pis'ma to EChAYa, **15** (10), 7 (1274). (in Russian).
- [14] N.N. Koval, O.V. Krysina, V.V. Shugurov. Minsk **25**, 1, 403 (2015).
- [15] S.V. Mikhailova. Structure and electronic properties of films of amorphous diamond-like carbon (a-C:H) modified by metal nanocrystals. Kazakh National. un-t im. al-Farabi, Almaty (2017).
- [16] A. Ferrari, J. Robertson. Phil. Trans. R. Soc. Lond. Ser. Math. Phys. Eng. Sci. **362**, 2477 (2004).
- [17] W.M. Haynes. CRC Handbook of Chemistry and Physics. 97th ed. CRC Press, (2016).
- [18] A. Evtukh, V.G. Litovchenko, M. Strikha, A. Kurchak, O. Yilmazoglu, H. Hartnagel. Ukr. J. Phys., **62**, 526 (2017).
- [19] M.O. Aboelfotoh. Solid State Electron. **34**, 1, 51 (1991).
- [20] S. Pal, R. Kumar Tiwari, D. Chandra Gupta, A. Singh Verma. J. Mater. Phys. Chem. **2**, 2, 20 (2014).
- [21] S. Miyagawa, S. Nakao, J. Choi, M. Ikeyama, Y. Miyagawa. New Diam. Front. Carbon Technol. **16**, 1, 6 (2006).